# Base Pairing of 8-Aza-7-deazapurine-2,6-diamine Linked *via* the N(8)-Position to the DNA Backbone: Universal Base-Pairing Properties and Formation of Highly Stable Duplexes when Alternating with dT

by **Junlin He** and **Frank Seela***

Laboratorium für Organische und Bioorganische Chemie, Institut für Chemie, Universität Osnabrück, Barbarastr. 7, D-49069 Osnabrück

The unusually $N^8$-glycosylated pyrazolo[3,4-*d*]pyrimidine-4,6-diamine 2′-deoxyribonucleoside (**3**) was synthesized and converted to the phosphoramidite **11**. Oligonucleotides were prepared by solid-phase synthesis, and the base pairing of compound **3** was studied. In non-self-complementary duplexes containing compound **3** located opposite to the four canonical DNA constituents, strong base pairs are formed that show ambiguous pairing properties. The self-complementary duplex d(**3**-T)$_6$ (**34**·**34**) is significantly more stable than d(A-T)$_6$.

**Introduction.** – Earlier, it was shown that $N^8$-glycosylated 8-aza-7-deazaadenine (= pyrazolo[3,4-*d*]pyrimidin-4-amine) 2′-deoxyribonucleoside (**1**) [1–3] acts as a universal nucleoside when positioned opposite any of the four canonical DNA constituents [4]. It forms an unusually stable base pair with thymidine when it replaces 2′-deoxyadenosine within d(A-T)$_6$ ($\Delta T_m = 1.3°$/**1**·dT) (*Fig. 1*) [2]. Its $N^9$-linked isomer **4** does not have such a property [5] (purine numbering is used throughout the *Results and Discussion* section). Recently, the base-pairing capability of the related $C^8$-linked 7-deazaguanosine (**2**) was reported [6]. It shows a base recognition pattern similar to that of 2′-deoxyisoguanosine but one different from the regularly glycosylated 2′-deoxyguanosine. Strong base pairs between compound **2** and 2′-deoxy-5-methylisocytidine are observed in DNA duplexes with antiparallel chain orientation. To the contrary, compound **2** forms base pairs of similar stability with dC in parallel DNA. From model building, it was anticipated that compound **3** would exhibit pairing properties similar to those of nucleoside **1**. However, due to the presence of the additional 2-amino group, a stronger base pair with dT was expected. We now report the synthesis of a phosphoramidite building block **11**, prepared from nucleoside **3**, and its base-pairing properties in self-complementary and non-self-complementary oligonucleotide duplexes. The $T_m$ data obtained from hybridization experiments will be compared with those of compound **1** [5]. Moreover, the potential of this compound as a universal nucleoside is studied. Ambiguous base pairing is not found for the $N^9$-glycosylated nucleosides **5** and **6** [7][8].

**Results and Discussion.** – 1. *Monomers.* The sugar-protected compound **7** [9] was used as the starting material. It was detoluoylated to yield nucleoside **8**. Next, the isopropoxy group of **8** was replaced by an amino group (25% aqueous $NH_3$ solution, 60°, 4d) to give nucleoside **3**. For oligonucleotide solid-phase synthesis, the amino

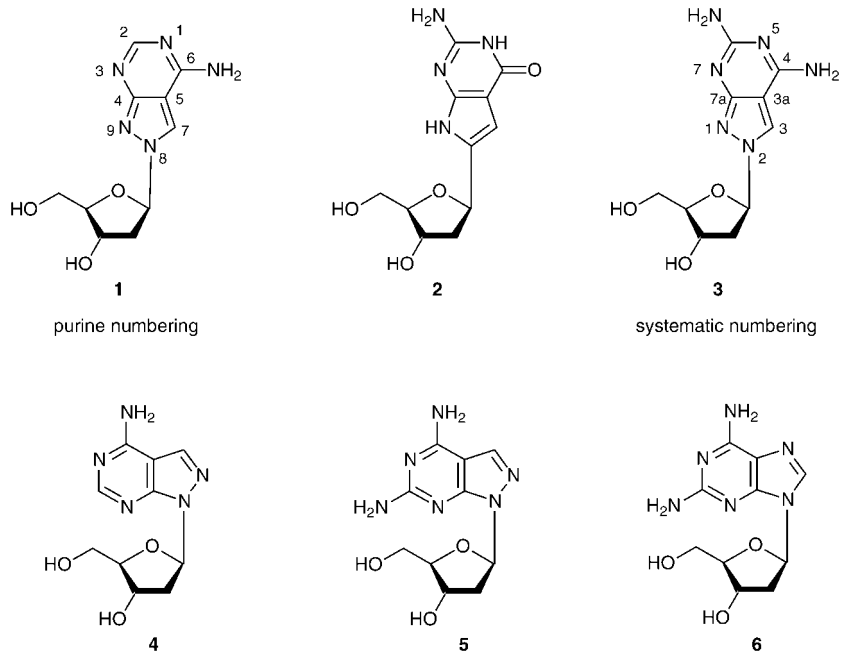


Fig. 1. $N^8$- *and* $N^9$-*Glycosylated nucleobases*

groups of **3** were protected. It has been reported that the reactivities of the two amino groups of **5** and **6** are different, which complicated the synthesis of the oligonucleotide building blocks [10]. Various protecting groups have been studied. As the isobutyryl residue was already successfully used for the protection of compound **5**, the same residues were employed in the case of **3** [10–12]. The protocol of transient protection was employed [13] (*Scheme 1*). The two isobutyrylation products isolated are compound **9a** carrying three isobutyryl residues (42% yield) and compound **9b** carrying one isobutyryl residue at each amino group (20%). The monoprotected **9c** was not obtained. The triisobutyrylated **9a** was chosen for further experiments. Syntheses of the $(MeO)_2$Tr derivative **10** and of the phosphoramidite **11** were performed by standard protocols (*Scheme 1*) [14].

The position of glycosylation as well as the anomeric configuration of compound **3** were assigned unambiguously by $^{13}$C-NMR chemical shifts as well as by NOE difference spectra (*Scheme 2*). According to our definition [4], the orientation of the base on $N^8$-glycosylated nucleosides is '*anti*' when the distance between H–C(1′) and H–C(7) is minimal and '*syn*' when this distance is maximal (*Scheme 2,b*). This is different to the definition of $N^9$-linked nucleosides, in which the orientation of the base is '*syn*' when the distance between H–C(1′) and H–C(8) is minimal and '*syn*' when this distance is maximal. As an NOE effect between H–C(7) and H–C(1′) was observed, the nucleoside **3** adopts a 55% '*anti*' population, which is similar to that of nucleoside **1** (66% '*anti*') [4].

*Scheme 1*

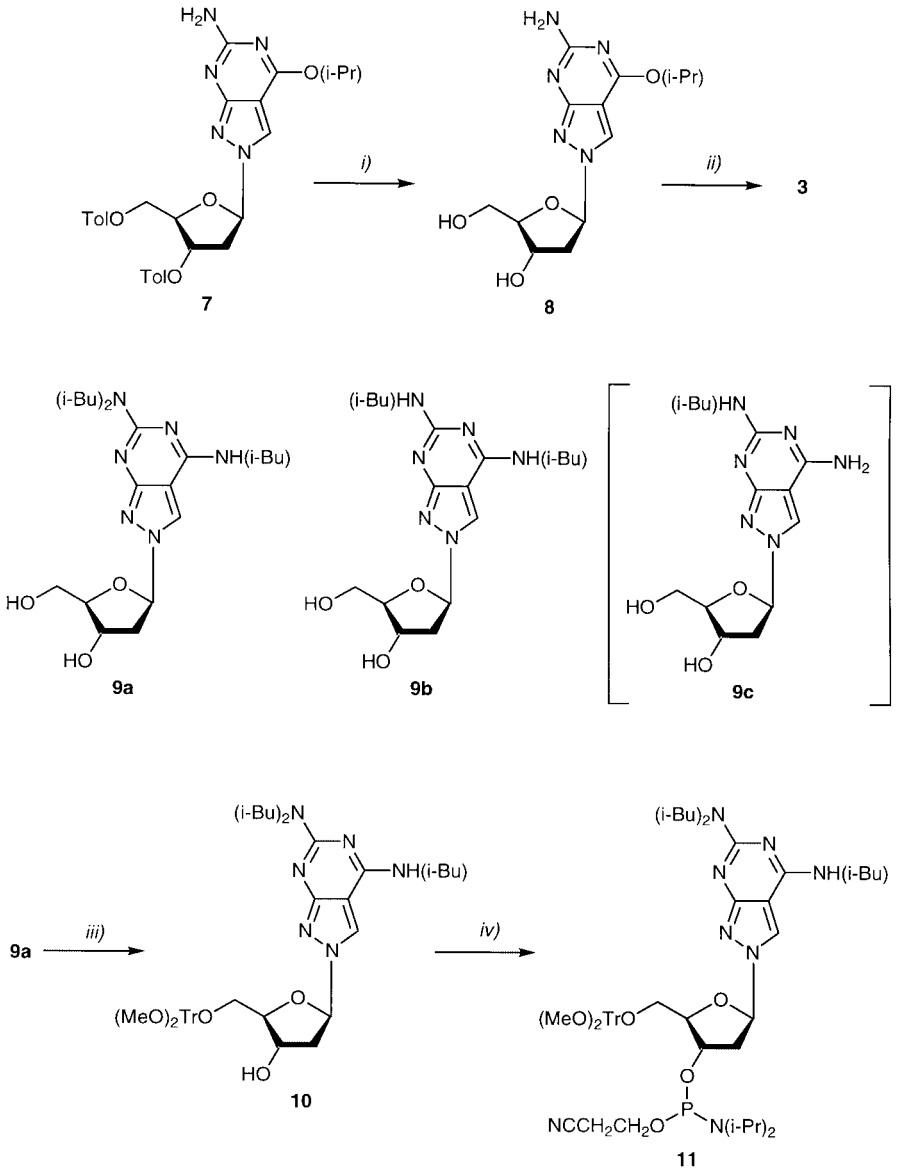


*i*) 0.1M MeONa/MeOH, 45°, 1 h. *ii*) 25% aq. $NH_3$ soln., 60°, 4 d. *iii*) $(MeO)_2TrCl$, pyridine, r.t., 4 h. *iv*) 2-Cyanoethyl diisopropylphosphoramidochloridite, $CH_2Cl_2$, r.t., 30 min.

Irradiation of H–C(1′) of **3** results in a strong NOE on H–C(7) (6.3%) besides weaker NOEs on H–C(2′) (4.8%) and H–C(4′) (1%) (*Scheme 2,a*). On the other hand, irradiation of H–C(7) gives an NOE on H–C(1′) (6.3%) (*Scheme 2,b*). The NOEs on H–C(2′) and H–C(4′) established the $\beta$-D configuration, while the NOE on H–C(7) indicated that the sugar moiety is connected *via* N(8). The '*syn*'/'*anti*' population of the nucleoside **3** was calculated by means of a calibration graph published earlier for regularly linked nucleosides [15].

Scheme 2. *NOE Data of the* 'anti' *States of Nucleoside* **3**

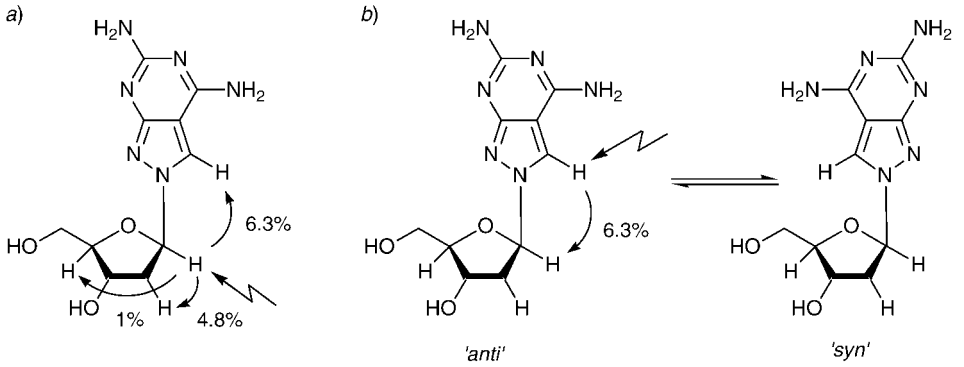


The sugar conformation was studied by means of the vicinal $^3J$(H,H) coupling constants of the $^1$H-NMR spectra measured in $D_2O$ applying the PSEUROT program [16]. The *S*-conformer populations of all pyrazolo[3,4-*d*]pyrimidine nucleosides **1** and **3**–**5** (56–63%) are lower compared to that of 2′-deoxyadenosine (72%) [17]. For nucleoside **3**, the *S*-population is somewhat higher than for nucleoside **1** (61 *vs.* 56%). The conformation about the C(4′)–C(5′) bond ($\gamma^{(+)g} \rightleftharpoons \gamma^{t} \rightleftharpoons \gamma^{(-)g}$) of nucleoside **3** shows no preference for either the $+sc$ (43%) or the $-sc$ (40%) rotamer population, which is analogous to the results with other pyrazolo[3,4-*d*]pyrimidine nucleosides [4].

To study the stability of the protecting groups, the deprotection of compounds **9a** and **9b** was monitored by UV spectroscopy in 25% aqueous $NH_3$ solution at 40° (**9a** at 328 nm; **9b** at 250 nm; at these two wavelengths, greatest absorbance changes during hydrolysis were observed and thus used for monitoring). As the stepwise deprotection was difficult to follow UV-spectrophotometrically, the reaction products were identified by HPLC (*Fig. 2*,*a* for **9a**, and *Fig. 2*,*b* for **9b**). In both cases (after 50 min for **9a** and 150 min for **9b**), the deprotection resulted in the formation of the unprotected nucleoside **3** and a monoprotected derivative **9c**. The latter was not assigned unambiguously. *Figs. 2*,*c* and *d*, show the HPLC profiles of the hydrolysis products together with their starting materials **9a** and **9b**. From these observations, it is apparent that an isobutyryl residue protecting the 6-amino group is much more labile than that protecting the 2-amino function [10][11]. As indicated by HPLC, all protecting groups are completely removed under the conditions of oligonucleotide deprotection (60°, 25% aqueous $NH_3$ solution, overnight). The stability of nucleoside **3** was also studied in 1N HCl at room temperature. When the reaction was followed by HPLC for 1 h (for conditions, see *Fig. 2*), no significant decomposition was observed.

All compounds were characterized by $^1$H- and $^{13}$C-NMR spectra. The assignments of the $^{13}$C-NMR resonances were made on the basis of $^1$H,$^{13}$C coupling constants, which were determined from gated-decoupled spectra (*Tables 1* and *2*). The $^{13}$C-NMR chemical shifts of C(2), C(4), and C(6) of compound **3** are tentatively assigned. The $^{13}$C-NMR chemical shift of C(7), being almost identical to that of compound **1**, confirmed N(8) as the glycosylation site, in agreement with the NOE-difference spectra. Next, the position of the isobutyryl residues of the triisobutyrylated derivative **9a** was determined. For this purpose, the $^2J$ and $^3J$ $^1$H,$^{13}$C coupling constants of

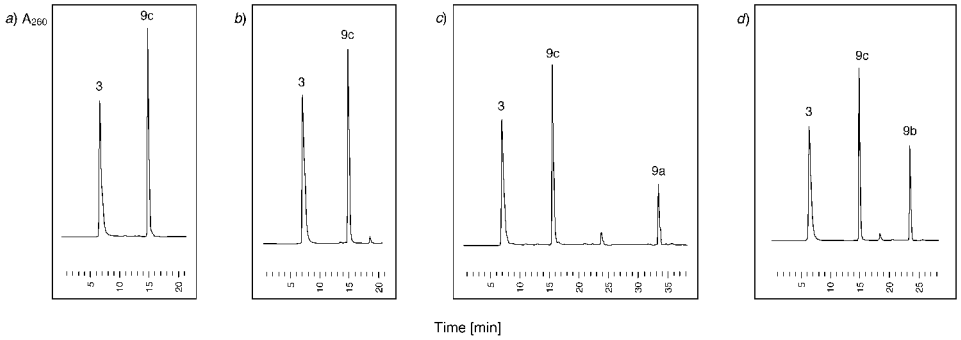


Fig. 2. *HPLC Profile of the deprotection* a) *of nucleoside* **9a** (25% aq. $NH_3$ soln., 40°, 50 min) *and* b) *of nucleoside* **9b** (25% aq. $NH_3$ soln., 40°, 150 min), c) *of the mixture of* **9a** *and its deprotection products, and* d) *of the mixture of* **9b** *and its hydrolysis products.* The HPLC was performed on an *RP-18* column (20 × 1 cm) with buffer *B* (see *Exper. Part*) and was monitored at 260 nm; flow rate 0.7 ml/min.

Table 1. *$^{13}$C-NMR Chemical Shifts of Pyrazolo[3,4-*d*]pyrimidine Nucleosides*[a])

| | C(2)[b]) C(6)[c]) | C(4)[b]) C(7a)[c]) | C(5)[b]) C(3a)[c]) | C(6)[b]) C(4)[c]) | C(7)[b]) C(3)[c]) | C(1′) | C(2′) | C(3′) | C(4′) | C(5′) | C=O, Me, CH |
|---|---|---|---|---|---|---|---|---|---|---|---|
| **1** [1] | 156.7 | 159.6 | 101.4 | 159.5 | 124.0 | 90.5 | [d]) | 70.7 | 88.4 | 62.1 | |
| **3** | 162.7[e]) | 162.3[e]) | 97.6 | 159.6[e]) | 124.3 | 90.1 | 40.4 | 71.0 | 88.3 | 62.5 | |
| **4** [1] | 156.2 | 153.8 | 100.6 | 158.2 | 133.2 | 87.7 | 38.1 | 71.2 | 84.2 | 62.6 | |
| **5** [4] | 156.9 | 158.3 | 95.5 | 162.7 | 133.3 | 87.4 | 38.0 | 71.3 | 83.3 | 62.7 | |
| **8** | 161.5 | 164.1 | 97.8 | 163.2 | 123.7 | 90.1 | [d]) | 70.5 | 88.2 | 61.9 | 21.7, 68.4 |
| **9a** | 155.6 | 161.4 | 101.6 | 156.4 | 130.1 | 91.0 | [d]) | 70.5 | 88.7 | 61.9 | 176.9, 179.6 |
| **9b** | 154.8 | 161.3 | 100.6 | 155.2 | 129.1 | 90.6 | [d]) | 70.7 | 88.6 | 62.1 | 175.3, 176.8 |
| **10** | 155.6 | 161.4 | 101.8 | 156.5 | 130.4 | 90.7 | 40.5 | 70.4 | 86.5 | 64.3 | 177.0, 179.5 |

[a]) Measured in ($D_6$)DMSO. [b]) Purine numbering. [c]) Systematic numbering. [d]) Superimposed by DMSO. [e]) Tentative.

Table 2. *$^{13}$C,$^{1}$H-Coupling Constants* [Hz] *of Pyrazolo[3,4-*d*]pyrimidine-4,6-diamine Nucleosides*[a])

| | Coupling constant | **1** | **3** | **9a** |
|---|---|---|---|---|
| C(2)[b]) (C(6)[c])) | $^{1}J$(C(2), H–C(2)) | 194.6 | | |
| C(4)[b]) (C(7a)[c])) | $^{3}J$(C(4), H–C(7)) | 7.4 | 7.1 | 7.3 |
| C(7)[b]) (C(3)[c])) | $^{1}J$(C(7), H–C(7)) | 194.1 | 191.4 | 203.4 |
| | $^{3}J$(C(7), H–C(1′)) | 1.6 | 1.6 | 1.4 |
| C(5)[b]) (C(3a)[c])) | $^{2}J$(C(5), H–C(7)) | 7.1 | 7.7 | 6.9 |
| | $^{3}J$(C(5), H–N(6)) | 4.6 | 3.9 | 4.4 |
| C(1′) | $^{1}J$(C(1′), H–C(1′)) | 167.5 | 165.4 | 169.3 |
| | $^{2}J$(C(1′), H–C(2′)) | 7.3 | 6.9 | |
| | $^{1}J$(C(1′), H–C(3)) | 3.3 | 2.6 | |
| C(4′) | $^{1}J$(C(4′), H–C(4′)) | 146.9 | 146.9 | 146.9 |
| C(3′) | $^{1}J$(C(3′), H–C(3′)) | 147.6 | 147.6 | 151.0 |
| C(5′) | $^{1}J$(C(5′), H–C(5′)) | 139.6 | 139.9 | 138.9 |

[a]) Measured in $D_2O$ at 303 K, [b]) Purine numbering. [c]) Systematic numbering.

compounds **1**, **3**, and **9a** (*Fig. 3*) were compared (*Table 2*). Nucleoside **3** shows a *dt* for C(5), due to couplings with H–C(7) and the two protons of the 6-amino group. Analogous couplings were also observed for nucleoside **1**. In compound **9a**, the signal of C(5) was a *dd*, due to couplings with one proton of the amide moiety and H–C(7). This indicates that only one isobutyryl group is attached to the 6-amino function of **9a**, while the 2-amino group carries two isobutyryl residues.

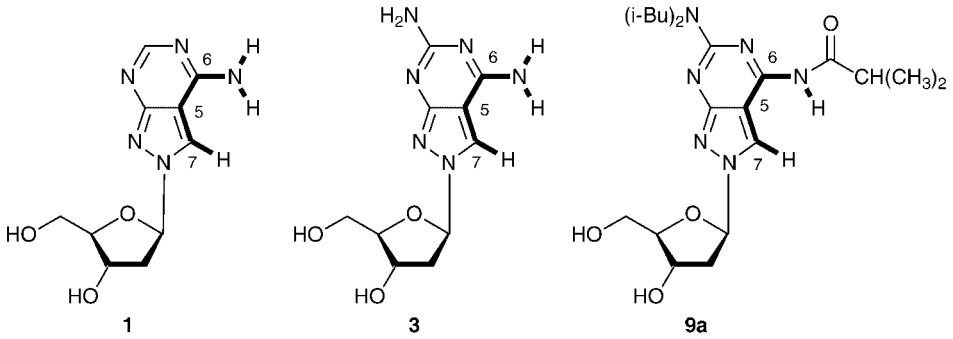


Fig. 3. *$^{13}C,^{1}H$-Coupling paths of nucleosides* **1**, **3**, *and* **9a**

2. *Oligonucleotides.* 2.1. *Synthesis.* The oligonucleotides **12**–**38** (*Tables 3–7*) were prepared by solid-phase synthesis by means of phosphoramidite chemistry. The coupling efficiency was always higher than 95%. Deprotection of the oligomers was conducted in 25% aqueous ammonia at 60°. Reversed-phase HPLC was applied for the purification (see *Exper. Part*). The composition of the oligomers was verified after tandem hydrolysis with snake-venom phosphodiesterase/alkaline phosphatase by HPLC analysis as described. The composition of oligonucleotides **15** (*Fig. 4,a*) and **38** (*Fig. 4,b*) was analyzed by reversed-phase HPLC after enzymatic digestion; the relative ratios of all nucleosides were in agreement with that calculated for the oligonucleotides. The retention time of the canonical nucleosides and compound **5** (*Fig. 4,c*) were used as reference. The chromatographic mobility of the $N^8$-glycosylated nucleoside **3** is greater than that of the $N^9$-compound **5** (*Fig. 4,c*). MALDI-TOF Mass spectrometry indicated that the masses of the oligomers were in agreement with the calculated values (see *Exper. Part*).

2.2. *Base-Pairing Properties.* To study the base-pairing properties of nucleoside **3**, non-self-complementary and self-complementary oligonucleotides were prepared that were derived from the duplexes 5′-d(TAG GTC AAT ACT)·3′-d(ATC CAG TTA TGA) (**12**·**13**), [5′-d(A-T)$_6$]$_2$ (**31**·**31**), [5′-d(A)$_6$-d(T)$_6$] (**35**·**35**), or [5′-d(T)$_6$-d(A)$_6$]$_2$ (**36**·**36**). The dA residues were partly or fully replaced by the $N^8$-nucleoside **3**, or by the nucleosides **1** or **4** for comparison.

2.2.1. *Stability of Non-Self-Complementary Duplexes.* At first, the nucleoside **3** was introduced into the non-self-complementary duplex **12**·**13** opposite to dT. According to *Table 3*, the $T_m$ decrease is moderate when two modified residues are positioned in the flanking region (see **15**·**17**) and stronger when they are located in the center of the duplex (see **14**·**15** or **15**·**16**) – phenomena well-known from other modified duplexes [10]. A particularly strong decrease is observed when the central dA-residues are

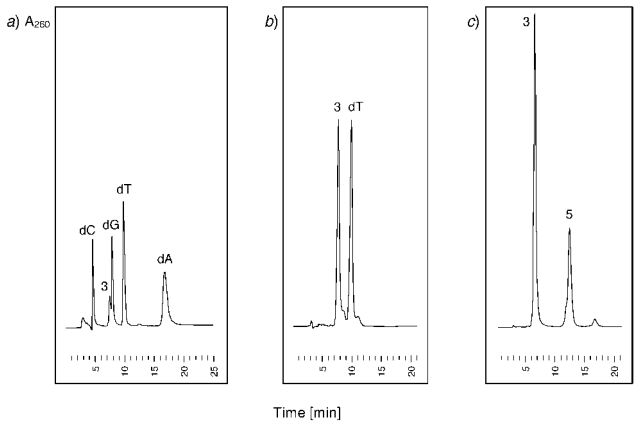


Fig. 4. *HPLC Profile of the enzymatic hydrolysis* a) *of oligonucleotide* **15** *and* b) *of oligonucleotide* **38** *by snake-venom phosphodiesterase followed by alkaline phosphatase in 0.1*M Tris · *HCl buffer* (pH 8.3); c) *HPLC profile of nucleosides* **3** *and* **5**. Conditions, see *Exper. Part.*

Table 3. $T_m$ *Values and Thermodynamic Data of Antiparallel-Strand Oligonucleotide Duplexes Containing the Nucleoside* **3** *Located Opposite dT*[a])

| | $T_m$ [°] | $\Delta H°$ [kcal/mol] | $\Delta S°$ [cal/mol K] | $\Delta G°_{310}$ [kcal/mol] |
|---|---|---|---|---|
| 5′-d(TAG GTC AAT ACT)-3′ (**12**) [11]<br>3′-d(ATC CAG TTA TGA)-5′ (**13**) | 50 (47) | – 90 | – 252 | – 12.0 |
| 5′-d(TAG GTC A**3**T ACT)-3′ (**14**)<br>3′-d(ATC C**3**G TTA TGA)-5′ (**15**) | 39 | – 72 | – 204 | – 8.1 |
| 5′-d(TAG GTC **33**T ACT)-3′ (**16**)<br>3′-d(ATC C**3**G TTA TGA)-5′ (**15**) | 40 | – 81 | – 234 | – 8.4 |
| 5′-d(T**3**G GTC AAT **3**CT)-3′ (**17**)<br>3′-d(ATC C**3**G TTA TGA)-5′ (**15**) | 45 | – 79 | – 225 | – 9.6 |
| 5′-d(TAG GTC A**3**T ACT)-3′ (**14**)<br>3′-d(ATC C**3**G TT**3** TGA)-5′ (**18**) | 30 | – 60 | – 174 | – 6.2 |

[a]) Measured at 260 nm in 1M NaCl, 100 mM $MgCl_2$, and 60 mM Na cacodylate (pH 7.0) with 10 μM oligonucleotide concentration. Data in parentheses were measured in 100 mM NaCl, 10 mM $MgCl_2$, and 10 mM Na cacodylate (pH 7.0) with 10 μM oligonucleotide concentration. The standard errors of thermodynamic data for $\Delta H°$ and $\Delta S°$ obtained from the curve fitting are within 15%.

replaced in the oligomer **13** (see **14** · **18**). This phenomenon is a structural feature of the sequence and has also been observed in other cases. When duplexes containing nucleoside **3** are compared with those having the abasic residue d**S** [4] (d**S** = 1,2-dideoxyribose; *Table 4*), the stabilization of the base is obvious. The effects of the diamino compound **3** are in the range of the 'adenine nucleoside' **1**. However, compound **3** gives higher $\Delta H$ values than compound **1**. An increasing number of **3**-residues leads to a decrease of the $T_m$ value.

The CD spectra of these duplexes are similar to those of the unmodified compounds (*Fig. 5,a*). These findings indicate that the change of the glycosylation position can meet the spatial demand for the base pairing within an appropriate distance to form H-

Table 4. *Comparison of the Influence of Nucleosides* **1**, **3**, *and d***S** *on the Duplex Stability*[a])[b])[c])

| | $T_m$ [°] | $\Delta H^\circ$ [kcal/mol] | $\Delta S^\circ$ [cal/mol K] | $\Delta G^\circ_{310}$ [kcal/mol] |
|---|---|---|---|---|
| 5′-d(TAG GTC A**3**T ACT)-3′ (**14**)<br>3′-d(ATC CAG TTA TGA)-5′ (**13**) | 44 (43) | – 82 | – 233 | – 9.6 |
| 5′-d(TAG GTC A**S**T ACT)3′ (**19**)<br>3′-d(ATC CAG TTA TGA)-5′ (**13**) | 33 | – 47 | – 129 | – 7.0 |
| 5′-d(TAG GTC AAT ACT)-3′ (**12**)<br>3′-d(ATC C**3**G TTA TGA)-5′ (**15**) | 46 | – 88 | – 249 | – 10.1 |
| 5′-d(TAG GTC AAT ACT)-3′ (**12**)<br>3′-d(ATC C**1**G TTA TGA)-5′ (**20**) | 46 (42) | – 77 | – 217 | – 9.8 |
| 5′-d(TAG GTC AAT ACT)-3′ (**12**)<br>3′-d(ATC C**S**G TTA TGA)-5′ (**21**) | 33 | – 61 | – 174 | – 6.9 |
| 5′-d(TAG GTC **33**T ACT)-3′ (**16**)<br>3′-d(ATC CAG TTA TGA)-5′ (**13**) | 45 | – 91 | – 261 | – 10.2 |
| 5′-d(TAG GTC **11**T ACT)-3′ (**22**)<br>3′-d(ATC CAG TTA TGA)-5′ (**13**) | 44 | – 79 | – 224 | – 9.5 |
| 5′-d(T**3**G GTC AAT **3**CT)-3′ (**17**)<br>3′-d(ATC CAG TTA TGA)-5′ (**13**) | 49 | – 88 | – 248 | – 11.1 |
| 5′-d(T**1**G GTC AAT **1**CT)-3′ (**23**)<br>3′-d(ATC CAG TTA TGA)-5′ (**13**) | 48 | – 80 | – 224 | – 10.5 |
| 5′-d(TAG GTC AAT ACT)-3′ (**12**)<br>3′-d(ATC C**3**G TT**3** TGA)-5′ (**18**) | 39 | – 63 | – 177 | – 7.9 |
| 5′-d(TAG GTC AAT ACT)-3′ (**12**)<br>3′-d(ATC C**1**G TT**1** TGA)-5′ (**24**) | 38 | – 57 | – 158 | – 7.8 |
| 5′-d(T**3**G GTC AAT **3**CT)-3′ (**17**)<br>3′-d(ATC C**3**G TT**3** TGA)-5′ (**18**) | 39 | – 62 | – 173 | – 7.9 |
| 5′-d(T**1**G GTC AAT **1**CT)-3′ (**23**)<br>3′-d(ATC C**1**G TT**1** TGA)-5′ (**24**) | 33 | – 48 | – 122 | – 6.8 |
| 5′-d(TAG GTC **33**T ACT)-3′ (**16**)<br>3′-d(ATC C**3**G TT**3** TGA)-5′ (**18**) | 32 | – 68 | – 197 | – 6.5 |
| 5′-d(TAG GTC **11**T ACT)-3′ (**22**)<br>3′-d(ATC C**1**G TT**1** TGA)-5′ (**24**) | 27 | – 45 | – 126 | – 6.2 |

[a]) See *Table 3*. [b]) d**S** = 1,2-dideoxyribose. [c]) The thermodynamic data of duplexes containing nucleoside **1** and d**S** were from [4].

bonds and base-stacking interactions. However, an additional 2-amino group has almost no effect on the duplex stability. Obviously, tridentate base pairs are not formed.

Nucleoside **1** can pair with the four natural nucleosides without much penalty of stability [4]. It is acting as an universal nucleoside, behaving differently to its $N^9$-glycosylated counterpart **4**. To study those properties, the base pairing between **3** and the four canonical nucleosides were investigated in non-self-complementary duplexes (*Tables 5* and *6*). Nucleoside **1** and the abasic residue d**S** were also incorporated into the same positions to allow a comparison of data. When nucleoside **3** is located opposite to dC, dA, or dG (*Tables 5* and *6*), similar effects on the $T_m$ values are observed as found for **1**. Apparently, the additional 2-amino group contributes very little to the

Table 5. $T_m$ *Values and Thermodynamic Data of Antiparallel-Strand Oligonucleotides* **15** *and* **20** *Containing the Nucleosides* **1** *and* **3** *Located Opposite dT or Other Canonical Nucleosides*[a])[b])[c])

| | $T_m$ [°] | $\Delta H^\circ$ [kcal/mol] | $\Delta S^\circ$ [cal/mol K] | $\Delta G^\circ_{310}$ [kcal/mol] |
|---|---|---|---|---|
| 5′-d(TAG G**T**C AAT ACT)-3′ (**12**)<br>3′-d(ATC C**A**G TTA TGA)-5′ (**13**) | 50 | – 90 | – 252 | – 12.0 |
| 5′-d(TAG G**T**C AAT ACT)-3′ (**12**)<br>3′-d(ATC C**1**G TTA TGA)-5′ (**20**) | 46 | – 76 | – 212 | – 9.9 |
| 5′-d(TAG G**T**C AAT ACT)-3′ (**12**)<br>3′-d(ATC C**3**G TTA TGA)-5′ (**15**) | 46 | – 88 | – 249 | – 10.1 |
| 5′-d(TAG G**T**C AAT ACT)-3′ (**12**)<br>3′-d(ATC C**S**G TTA TGA)-5′ (**21**) | 33 | – 61 | – 174 | – 6.9 |
| 5′-d(TAG G**C**C AAT ACT)-3′ (**25**)<br>3′-d(ATC C**1**G TTA TGA)-5′ (**20**) | 46 | – 80 | – 225 | – 9.9 |
| 5′-d(TAG G**C**C AAT ACT)-3′ (**25**)<br>3′-d(ATC C**3**G TTA TGA)-5′ (**15**) | 42 | – 85 | – 244 | – 9.1 |
| 5′-d(TAG G**C**C AAT ACT)-3′ (**25**)<br>3′-d(ATC C**S**G TTA TGA)-5′ (**21**) | 35 | – 65 | – 187 | – 7.4 |
| 5′-d(TAG G**A**C AAT ACT)-3′ (**26**)<br>3′-d(ATC C**1**G TTA TGA)-5′ (**20**) | 45 | – 77 | – 217 | – 9.7 |
| 5′-d(TAG G**A**C AAT ACT)-3′ (**26**)<br>3′-d(ATC C**3**G TTA TGA)-5′ (**15**) | 43 | – 79 | – 226 | 9.1 |
| 5′-d(TAG G**A**C AAT ACT)-3′ (**26**)<br>3′-d(ATC C**S**G TTA TGA)-5′ (**21**) | 35 | – 76 | – 222 | – 7.2 |
| 5′-d(TAG G**G**C AAT ACT)-3′ (**27**)<br>3′-d(ATC C**1**G TTA TGA)-5′ (**20**) | 44 | – 73 | – 205 | – 9.4 |
| 5′-d(TAG G**G**C AAT ACT)-3′ (**27**)<br>3′-d(ATC C**3**G TTA TGA)-5′ (**15**) | 43 | – 77 | – 217 | – 9.4 |
| 5′-d(TAG G**G**C AAT ACT)-3′ (**27**)<br>3′-d(ATC C**S**G TTA TGA)-5′ (**21**) | 40 | – 71 | – 202 | – 8.6 |

[a]) See *Table 3*. [b])[c]) See *Table 4*.

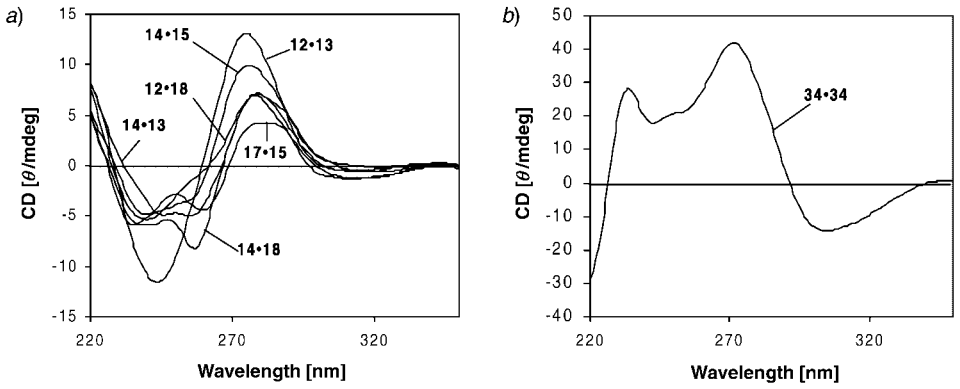


Fig. 5. *CD Spectra of helixes formed* a) *by non-self-complementary duplexes containing* **3** *and* b) *by the alternating duplex* **34**·**34**

Table 6. $T_m$ *Values and Thermodynamic Data of Antiparallel-Strand Oligonucleotides* **16** *and* **22** *Containing the Nucleosides* **1**, **3**, *or the Abasic Residue d***S** *Located Opposite the Canonical Nucleosides*[a])[b])[c])

| | $T_m$ [°] | $\Delta H^\circ$ [kcal/mol] | $\Delta S^\circ$ [cal/mol K] | $\Delta G^\circ_{310}$ [kcal/mol] |
|---|---|---|---|---|
| 5′-d(TAG GTC **11**T ACT)-3′ (**22**)<br>3′-d(ATC CAG **TT**A TGA)-5′ (**13**) | 44 | – 79 | – 224 | – 9.5 |
| 5′-d(TAG GTC **33**T ACT)-3′ (**16**)<br>3′-d(ATC CAG **TT**A TGA)-5′ (**13**) | 45 | – 91 | – 261 | – 10.2 |
| 5′-d(TAG GTC A**S**T ACT)-3′ (**19**)<br>3′-d(ATC CAG T**T**A TGA)-5′ (**13**) | 33 | – 47 | – 129 | – 7.0 |
| 5′-d(TAG GTC **11**T ACT)-3′ (**22**)<br>3′-d(ATC CAG **TC**A TGA)-5′ (**28**) | 42 | – 79 | – 225 | – 9.0 |
| 5′-d(TAG GTC **33**T ACT)-3′ (**16**)<br>3′-d(ATC CAG **TC**A TGA)-5′ (**28**) | 43 | – 85 | – 243 | – 9.2 |
| 5′-d(TAG GTC A**S**T ACT)-3′ (**19**)<br>3′-d(ATC CAG T**C**A TGA)-5′ (**28**) | 34 | – 52 | – 146 | – 7.1 |
| 5′-d(TAG GTC **11**T ACT)-3′ (**22**)<br>3′-d(ATC CAG **TA**A TGA)-5′ (**29**) | 42 | – 78 | – 223 | – 9.1 |
| 5′-d(TAG GTC **33**T ACT)-3′ (**16**)<br>3′-d(ATC CAG **TA**A TGA)-5′ (**29**) | 43 | – 86 | – 248 | – 9.2 |
| 5′-d(TAG GTC A**S**T ACT)-3′ (**19**)<br>3′-d(ATC CAG T**A**A TGA)-5′ (**29**) | 34 | – 51 | – 141 | – 7.2 |
| 5′-d(TAG GTC **11**T ACT)-3′ (**22**)<br>3′-d(ATC CAG **TG**A TGA)-5′ (**30**) | 39 | – 67 | – 190 | – 8.1 |
| 5′-d(TAG GTC **33**T ACT)-3′ (**16**)<br>3′-d(ATC CAG **TG**A TGA)-5′ (**30**) | 42 | – 79 | – 227 | – 8.8 |
| 5′-d(TAG GTC A**S**T ACT)-3′ (**19**)<br>3′-d(ATC CAG T**G**A TGA)-5′ (**30**) | 33 | – 48 | – 131 | – 7.0 |

[a]) See *Table 3*. [b])[c]) See *Table 4*.

Table 7. $T_m$ *Values and Thermodynamic Data of Alternating Self-Complementary Oligonucleotides Containing the Nucleosides* **1**, **3**, *and* **4** *Opposite d*T[a])

| | $T_m$ [°] | $\Delta H^\circ$ [kcal/mol] | $\Delta S^\circ$ [cal/mol K] | $\Delta G^\circ_{310}$ [kcal/mol] |
|---|---|---|---|---|
| [5′-d(ATATA TATATAT)-3′]$_2$ (**31**·**31**) [2] | 33(26) | – 49.5 | – 139.3 | – 6.3 |
| [5′-d(**4T4T4** T**4T4T4T**)-3′]$_2$ (**32**·**32**) [2] | 36 | – 63 | – 180 | – 7.2 |
| [5′-d(**1T1** T**1T** **1T1** T**1T**)-3′]$_2$ (**33**·**33**) [4] | 49(39) | – 74 | – 207 | – 9.6 |
| [5′-d(**3T3** T**3T** **3T3** T**3T**)-3′]$_2$ (**34**·**34**) | 58(55) | – 71.9 | – 191.9 | – 11.3 |
| [5′-d(AAA AAA TTT TTT)-3′]$_2$ (**35**·**35**) | 46(40) | | | |
| [5′-d(TTT TTT AAA AAA)-3′]$_2$ (**36**·**36**) | 33(29) | | | |
| [5′-d(**333 333** TTT TTT)-3′]$_2$ (**37**·**37**) | 42(48), 19(14) | | | |
| [5′-d(TTT TTT **333 333**)-3′]$_2$ (**38**·**38**) | 29(32) | | | |
| 5′-d(**333 333** TTT TTT)-3′ (**37**)<br>5′-d(TTT TTT **333 333**)-3′ (**38**) | 39(44) | | | |

[a]) See *Table 3*.

base-pair stability. In the case of two consecutive incorporations, compounds **1** and **3** lead to almost the same $T_m$ values. But duplexes containing compound **1** or **3** give much higher $T_m$ values than those incorporating the abasic residue d**S**. This means that interactive forces exist between **1** or **3** and the four canonical residues, such as H-bonding and/or base stacking. The CD spectra (*Fig. 6*) show that the mismatched base pairs do not disturb the duplex structure significantly. Thus, compound **3** has the potential of a universal nucleoside as it is found for nucleoside **1**.

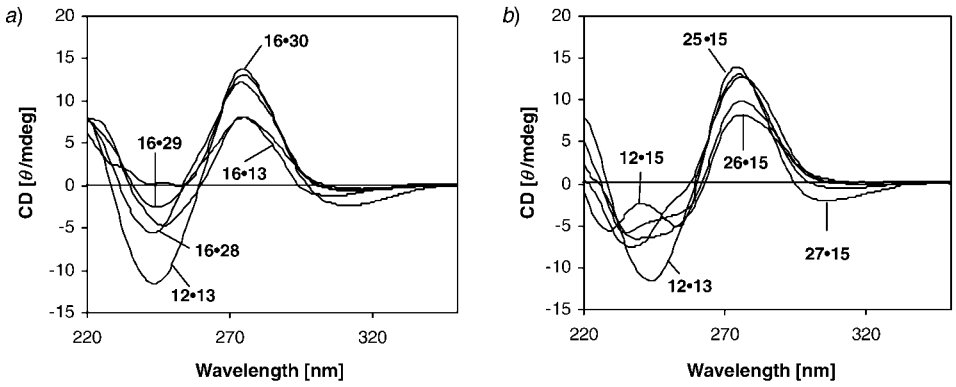


Fig. 6. *CD Spectra of duplexes containing nucleoside* **3** *opposite the four canonical nucleosides measured in* 1M *NaCl, 100 mM $MgCl_2$, and 10 mM Na cacodylate* (pH 7.0)

2.2.2. *Duplex Stability of Alternating Self-complementary Oligonucleotides.* Earlier, it was found that the oligomer d(**1**-T)$_6$ (**33**·**33**) forms a more stable duplex than the parent duplex d(**4**-T)$_6$ (**32**·**32**) incorporating the regularly $N^9$-glycosylated nucleoside [4]. Thus, it is expected that the replacement of dA by the diamino compound **3** increases the duplex stability further as a third H-bond might be formed as shown in base pair **VI** (**5**-dT; *Fig. 7*). According to *Table 7* the duplex **34**·**34** has a $T_m$ 9° higher than that of **33**·**33** and 25° higher than that of the unmodified **31**·**31**. This corresponds to a stabilization of each **3**-dT pair by 0.75° compared to that of the **1**-dT pair and by 2.1° compared to that of dA-dT. The duplex **32**·**32** (base pair **V**; *Fig. 7*) containing the regularly $N^9$-linked pyrazolo[3,4-*d*]pyrimidine nucleoside **4** is only slightly more stable than the parent duplex **31**·**31**. The CD spectrum of **34**·**34** is very similar to that of **33**·**33** both of them having a negative lobe around 308 nm, while the control duplex has a negative lobe around 245 nm [2][18]. This indicates that the incorporation of $N^8$-glycosylated nucleoside residues into duplexes with alternating dA*·dT results in an autonomous DNA. Apparently, the additional 2-amino group of the nucleoside **3** can form H-bonds in this particular duplex, and a tridendate base pair is formed.

The chain orientation of the alternating duplexes incorporating either compound **1** or **3** (**33**·**33** or **34**·**34**) (*Table 7*) can be antiparallel (**I** and **III**) or parallel (**II** and **IV**) (*Fig. 7*). However, the antiparallel duplex d(A-T)$_6$ (**31**·**31**) is more stable than the parallel one [19]. This might not be the case for the duplexes **33**·**33** and **34**·**34**, which can form an autonomous DNA structure with possibly much better stacked nucleobase residues. To clarify this problem, the block oligomers d(**3**)$_6$-(T)$_6$ (**37**·**37**) and d(T)$_6$-(**3**)$_6$ (**38**·**38**) as well as control duplexes (see **35**·**35** and **36**·**36**) were synthesized (*Table 7*).

Only in the antiparallel case, stable duplexes are expected, while in a parallel arrangement, rather labile species should be formed (maximally six instead of twelve base pairs). In the parallel case, a stable duplex is expected only when **37** is hybridized with **38**. The melting curves show unexpected profiles (*Fig. 8,a*). The duplex **38**·**38** gives a monophasic melting profile, while the melting profile of **37**·**37** is biphasic. Both modified duplexes show a higher $T_m$ value under low salt buffer concentration than under high salt concentration conditions (see *Table 3*), a phenomenon difficult to understand. Also the CD spectra show significant changes (*Fig. 8,b*). The CD spectrum of **38**·**38** looks exactly like that of the control duplex **36**·**36** (not shown), while the spectra of **37**·**37** and **37**·**38** are different from that of **38**·**38**. From these experiments, no definite conclusion about chain orientation can be drawn. However, it seems more likely that the base pair **3**-dT is of the *Watson-Crick* type with antiparallel chain orientation for the alternating and the block oligonucleotides. Otherwise, the rather high $T_m$ values of **37**·**37** and **38**·**38** cannot be explained.

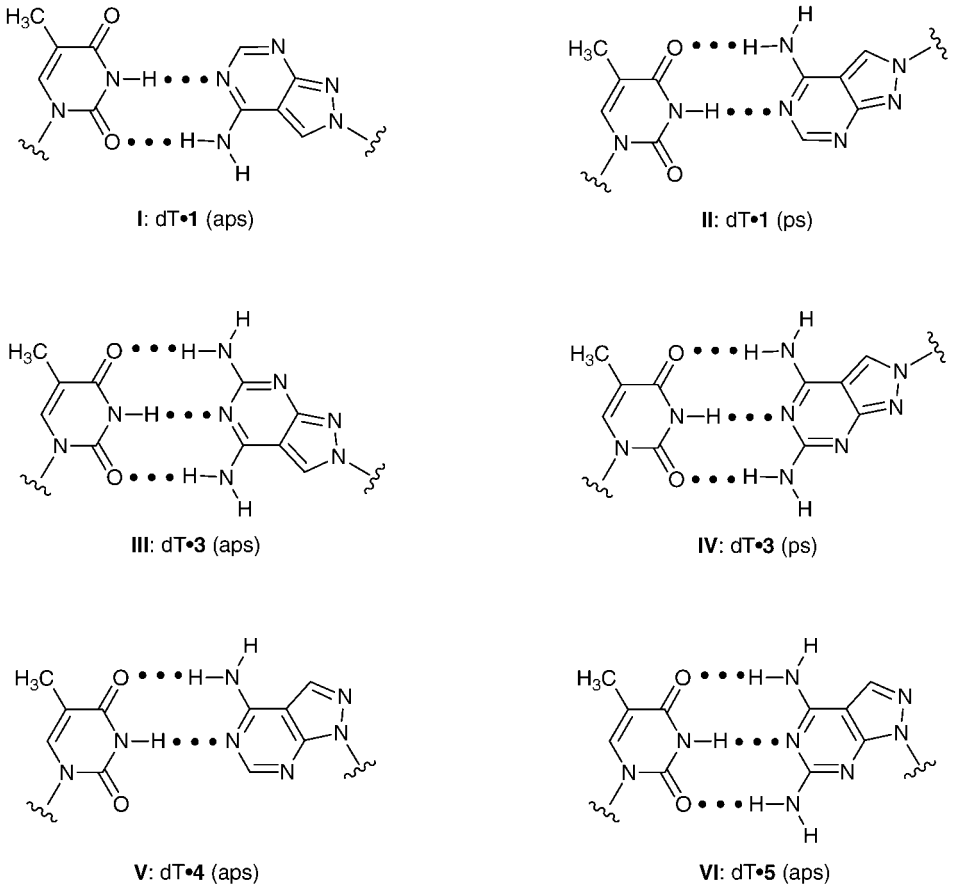


Fig. 7. *Base-pair motifs formed between nucleosides* **1**–**5** *and dT forming* Watson-Crick *or reverse* Watson-Crick *base pairs.* aps = antiparallel strand, ps = parallel strand.

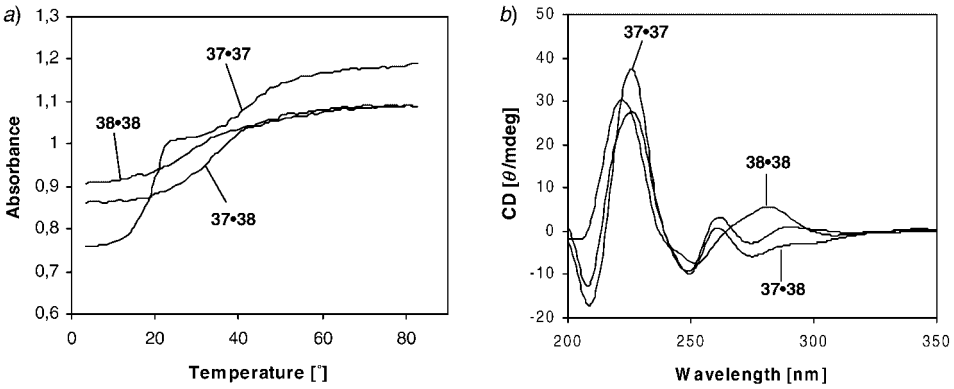


Fig. 8. a) *Melting profile of helices formed by the self-complementary block sequences* **37** *and* **38** (conditions, see *Exper. Part*). b) *CD spectra of duplexes* **37** · **37**, **38** · **38**, *and* **37** · **38**.

**Conclusions.** – The $N^8$-glycosylated nucleoside **3** shows similar base pairing behavior as compound **1** when it replaces dA residues in dA · dT base pairs. It shows ambiguous base pairing with the four canonical DNA constituents. The 2-amino group of **3** does not increase the base-pair stability. Thus, nucleoside **3** has the potential to be an universal nucleoside when it replaces only a few of the canonical nucleosides. The situation changes when the nucleoside **3** residue alternates with dT. In this case, the 12-mer duplex incorporating compound **3** is significantly more stable than that containing compound **1** or dA. Here, the additional 2-amino group of **3** has a great impact on the stability of the duplex structure. From these observations, it is concluded that only in the latter case does the 2-amino group participate in H-bonding with the 2-oxo group of dT.

We thank Dr. *H. Rosemeyer* for helpful discussions and Mr. *Yang He* for the NMR spectra. We also appreciate the syntheses of the oligonucleotides and their characterization by MALDI-TOF spectra by *E. Feiling*. Financial support by the *Deutsche Forschungsgemeinschaft* and the *Roche Diagnostics GmbH* is gratefully acknowledged.

## Experimental Part

*General*. See [10]. *Monomers.* Thin-layer chromatography (TLC): aluminium sheets, silica gel *60* $F_{254}$ (0.2 mm, *Merck*, Germany). Flash chromatography (FC): 0.4 bar; silica gel *60 H* (*Merck*, Darmstadt, Germany). Solvent systems for TLC and FC: $CH_2Cl_2$/MeOH 10:1 (*A*), $CH_2Cl_2$/MeOH 9:1 (*B*), $CH_2Cl_2$/MeOH 95:5 (*C*), $CH_2Cl_2$/acetone 10:1 (*D*), and $CH_2Cl_2$/acetone 9:1 (*E*). M.p.: *Büchi-SMP-20* apparatus (*Büchi*, Switzerland); uncorrected. NMR Spectra: *Avance-DPX-250* and *AMX-500* spectrometers (*Bruker*, Germany); $\delta$ values in ppm rel. to internal $SiMe_4$ ($^1H$, $^{13}C$) or external $H_3PO_4$ (85%), *J* in Hz. Microanalyses were performed by the *Mikroanalytisches Labor Beller* (Göttingen, Germany).

*Oligonucleotides.* Oligonucleotide synthesis: *ABI-392-DNA* synthesizer (*Applied Biosystems*, Weiterstadt, Germany) in the 'trityl-on' mode. Melting curves: *Cary-1-* or *Cary-1E*-UV/VIS spectrophotometers (*Varian*, Australia) equipped with a *Cary* thermoelectrical controller; the temp. was measured continuously in the reference cell with a Pt-*100* resistor, and the thermodynamic data of duplex formation were calculated with the program Meltwin 3.0 [20]. UV Spectra: *150-20* spectrometer (*Hitachi*, Japan); $\lambda_{max}(\varepsilon)$ in nm. CD Spectra: *Jasco-600* (*Jasco*, Japan) spectropolarimeter with thermostatically (*Lauda RCS-6* bath) controlled 1-cm cuvettes. The enzymatic hydrolysis of the oligomers was performed as described below [3], and the following extinction coefficients $\varepsilon_{260}$ were used: dA 15400, dG 11700, dT 8800, and dC 7300. Snake-venom phosphodiesterase (EC 3.1.15.1, *Crotallus adamanteus*) and alkaline phosphatase (EC 3.1.3.1, *E. coli*) were generous gifts from *Roche Diagnostics GmbH*, Germany. MALDI-TOF-MS: *Biflex-III* spectrometer (*Bruker Saxonia-Analytik GmbH*, Leipzig, Germany); results in *Table 8*.

Table 8. *Molecular Masses* ($MH^+$) *of Oligonucleotides Measured by MALDI-TOF Mass Spectrometry*

| | $MH^+$ (calc.) | $MH^+$ (found) |
|---|---|---|
| 5′-d(TAG GTC A**3**T ACT)-3′ (**14**) | 3659 | 3660 |
| 5′-d(AGT ATT G**3**C CTA)-3′ (**15**) | 3659 | 3662 |
| 5′-d(TAG GTC **33**T ACT)-3′ (**16**) | 3673 | 3675 |
| 5′-d(T**3**G GTC AAT **3**CT)-3′ (**17**) | 3673 | 3677 |
| 5′-d(AGT **3**TT G**3**C CTA)-3′ (**18**) | 3673 | 3676 |
| 5′-d(**3**T**3** T**3**T **3**T**3** T**3**T)-3′ (**34**) | 3732 | 3732 |
| 5′-d(**333 333** TTT TTT)-3′ (**37**) | 3732 | 3733 |
| 5′-d(TTT TTT **333 333**)-3′ (**38**) | 3732 | 3733 |

The synthesis was carried out on a 1-μmol scale with the monomer **11** and the 3′-phosphoramidites of $[(MeO)_2Tr]ib^2G_d$, $[(MeO)_2Tr]bz^6A_d$, $[(MeO)_2Tr]bz^4C_d$, and $[(MeO)_2Tr]T_d$. After the 'trityl-on' oligonucleotides were cleaved from the solid support, they were deprotected in 25% aq. $NH_3$ soln. for 12–15 h at 60°. Then, the purification was performed by reversed-phase HPLC (250 × 4 mm, *RP-18* column, *Merck*, Germany; gradient (*A*, 0.1M ($Et_3NH$)OAc (pH 7.0)/MeCN 95:5; *B*, MeCN): 3 min 20% *B* in *A*, 12 min 20–40% *B* in *A*, flow rate 1.0 ml/min). The purified 'trityl-on' oligonucleotides were treated with 2.5% $CHCl_2COOH/CH_2Cl_2$ for 5 min at r.t. to remove the 4,4′-dimethoxytrityl residues. The detritylated oligomers were purified again by reversed-phase HPLC (gradient: 20 min 0–20% *B* in *A*, flow rate 1 ml/min). The oligomers were desalted on a short column (*RP-18*, silica gel): colorless solids, which were stored at −24°.

The composition of oligonucleotides was established as follows: The oligonucleotides were dissolved in 0.1M *Tris*·HCl buffer (pH 8.3, 200 μl), and treated with snake-venom phosphodiesterase (3 μl) at 37° for 45 min, and subsequently with alkaline phosphatase (3 μl) at 37° for another 30 min. The mixtures were analyzed by HPLC (*RP-18*, at 260 nm, gradient *A*, 0.7 ml/min) to give the ratio of nucleosides incorporated in the oligonucleotide. The composition analysis of oligonucleotides **15** and **38** is shown in *Fig. 4*.

*2-(2-Deoxy-β-*D-erythro-*pentofuranosyl)-4-isopropoxy-2*H-*pyrazolo[3,4-*d*]pyrimidin-6-amine* (**8**). The protected nucleoside 2-[2-deoxy-3,5-di-*O*-(*p*-toluoyl)-*β*-D-erythro-pentofuranosyl]-4-isopropoxy-2*H*-pyrazolo[3,4-*d*]pyrimidin-6-amine (**7**) [9] (7.5 g, 13.8 mmol) was suspended in 0.1M $^i$PrONa/$^i$PrOH (400 ml), stirred, and heated gently (45°) for 1 h (TLC monitoring). The mixture was neutralized with AcOH and evaporated. The residue was dissolved in MeOH (*ca.* 50 ml). The soln. was adsorbed on silica gel (20 g); this material was loaded on top of a silica gel column (7 cm × 30 cm) and submitted to FC (6 cm × 30 cm, *A*). The main zone furnished **8** (3.0 g, 71%). Colorless solid. $R_f$ (*B*) 0.38. $^1$H-NMR ((D$_6$DMSO): 1.34 (*m*, *Me*$_2$CH); 2.30 (*m*, 1 H–C(2′)); 2.61 (*m*, 1 H–C(2′)); 3.58 (*m*, 2 H–C(5′)); 3.87 (*m*, H–C(4′)); 4.39 (*m*, H–C(3′)); 5.04 (*m*, OH–C(5′)); 5.28 (*m*, OH–C(3′)); 5.47 (*m*, Me$_2$*CH*); 6.15 (*t*, *J* = 6.0, H–C(1′)); 6.39 (*s*, NH); 8.41 (*s*, H–C(7)).

*2-(2-Deoxy-β-*D-erythro-*pentofuranosyl)-2*H-*pyrazolo[3,4-*d*]*pyrimidine-4,6-diamine* (**3**). A suspension of **8** (3.1 g, 10 mmol) in 25% aq. $NH_3$ soln. was heated in an autoclave at 60° for 4 d under stirring. The mixture was concentrated to a small volume, MeOH (100 ml) was added, and the soln. was adsorbed on silica gel (10 g). FC (silica gel, 6 × 20 cm, *A*) gave **3** (2.3 g, 86%). White solid. $R_f$ (*B*) 0.48. UV (MeOH): 225 (25000), 264 (9200), 295 (7600). $^1$H-NMR ((D$_6$)DMSO): 2.30 (*m*, 1 H–C(2′)); 2.58 (*m*, 1 H–C(2′)); 3.53 (*m*, 2 H–C(5′)); 3.88 (*m*, H–C(4′)); 4.40 (*m*, H–C(3′)); 5.09 (*m*, OH–C(5′)); 5.30 (*m*, OH–C(3′)); 5.79 (*s*, $NH_2$); 6.15 (*t*, *J* = 5.88, H–C(1′)); 7.21 (br., $NH_2$), 8.23 (*s*, H–C(7)). Anal. calc. for $C_{10}H_{14}N_6O_3$ (266.26): C 45.11, H 5.30, N 31.56; found: C 45.21, H 5.23, N 31.19.

*Isobutyrylation of* **3**. Compd. **3** (0.9 g, 3.38 mmol) was co-evaporated with anh. pyridine (3 times) and then dissolved in anh. pyridine (15 ml). $Me_3SiCl$ (2.16 ml, 17.0 mmol) was added to the soln. while stirring for 15 min at r.t. Then, isobutyric anhydride (3.56 ml, 21.5 mmol) was added, and stirring was continued for 3 h. The mixture was cooled in an ice-bath and diluted with cold $H_2O$ (6 ml). After 5 min, aq. 25% $NH_3$ soln. (6 ml) was added and the soln. stirred for 30 min. The mixture was evaporated and co-evaporated with toluene (3 times). The residue was purified by FC (*A*): fast migrating **9a** (0.57 g, 42%) and slow migrating **9b** (0.27 g, 20%).

*2-(2-Deoxy-β-*D-erythro-*pentofuranosyl)-*N$^4$,N$^6$,N$^6$-*triisobutyryl-2*H-*pyrazolo[3,4-*d*]*pyrimidine-4,6-diamine* (**9a**): Colorless amorphous solid. $R_f$ (*B*) 0.38. UV (MeOH): 276 (10850), 302 (7600). $^1$H-NMR ((D$_6$)DMSO): 1.12 (*m*, *Me*$_2$CH); 2.42 (*m*, 1 H–C(2′)); 2.64 (*m*, 1 H–C(2′)); 2.92 (*m*, Me$_2$*CH*); 3.51, 3.61 (*m*, 2 H–C(5′)); 3.93 (*m*, H–C(4′)); 4.45 (*m*, H–C(3′)); 4.87 (*t*, *J* = 5.35, OH–C(5′)); 5.36 (*d*, *J* = 4.35, OH–C(3′)); 6.50 (*t*, *J* = 5.63, H–C(1′)); 9.12 (*s*, H–C(7)); 11.47 (*s*, NH); 7.27–7.94 (*m*, arom. H); 8.44 (*s*, H–C(7)). Anal. calc. for $C_{22}H_{32}N_6O_6$ (476.53): C 55.45, H 6.77, N 17.64; found: C 55.41, H 6.51, N 17.11.

*2-(2-Deoxy-β-*D*-*erythro*-pentofuranosyl)-*N$^4$,N$^6$*-diisobutyryl-2*H*-pyrazolo[3,4-*d*]pyrimidine-4,6-diamine* (**9b**): $R_f$ (*B*) 0.32. UV (MeOH): 239 (41600), 285 (10900). $^1$H-NMR ((D$_6$)DMSO): 1.13 (*m*, *Me*$_2$CH); 2.39 (*m*, 1 H–C(2′)); 2.61 (*m*, 1 H–C(2′)); 3.00 (*m*, Me$_2$C*H*); 3.50, 3.60 (*m*, 2 H–C(5′)); 3.91 (*m*, H–C(4′)); 4.44 (*m*, H–C(3′)); 4.92 (*t*, *J* = 5.50, OH–C(5′)); 5.33 (*d*, *J* = 4.40, OH–C(3′)); 6.41 (*t*, *J* = 5.65, H–C(1′)); 8.87 (*s*, H–C(7)); 10.08, 11.00 (*s*, NH). Anal. calc. for $C_{18}H_{26}N_6O_5$ (406.44): C 53.19, H 6.45, N 20.68; found: C 53.76, H 6.55, N 20.03.

*2-[2-Deoxy-5-*O*-(4,4′-dimethoxytrityl)-β-*D*-pentofuranosyl]-N$^4$,N$^6$,N$^6$-triisobutyryl-2*H*-pyrazolo[3,4-*d*]pyrimidine-4,6-diamine* (**10**). Compound **9a** (0.55 g, 1.15 mmol) was co-evaporated with anh. pyridine (3 times) and dissolved in pyridine (2.5 ml). (MeO)$_2$TrCl (0.6 g, 1.76 mmol) was added, and the mixture was stirred at r.t. for 3 h. The reaction was quenched by the addition of MeOH and the mixture evaporated and co-evaporated with toluene. FC (6 cm × 30 cm, *A*) furnished **10** (0.26 g, 29%). Colorless foam. $R_f$ (*C*) 0.3. UV (MeOH): 275 (13000), 305 (7600). $^1$H-NMR ((D$_6$)DMSO): 1.12 (*m*, 3 *Me*$_2$CH); 2.46 (*m*, 1 H–C(2′)); 2.72 (*m*, Me$_2$C*H*); 2.91 (*m*, 1 H–C(2′)); 3.08 (*m*, 2 H–C(5′)); 3.65, 3.68 (*s*, 2 MeO); 4.05 (*m*, H–C(4′)); 4.53 (*m*, H–C(3′)); 5.40 (*d*, *J* = 5.0, OH–C(3′)); 6.60 (*m*, H–C(1′)); 6.69–7.79 (*m*, arom. H); 9.17 (*s*, H–C(7)); 11.50 (*s*, NH). Anal. calc. for $C_{43}H_{50}N_6O_8$ (778.89): C 66.31, H 6.42, N 10.79; found: C 66.48, H 6.53, N 10.59.

*2-[2-Deoxy-5-*O*-(4,4′-dimethoxytrityl)-β-*D*-*erythro*-pentofuranosyl]-N$^4$,N$^6$,N$^6$-triisobutyryl-2*H*-pyrazolo[3,4-*d*]pyrimidine-4,6-diamine 3′-(2-Cyanoethyl Diisopropylphosphoramidite)* (**11**). To a soln. of **10** (0.6 g, 0.77 mmol) in anh. $CH_2Cl_2$ (30 ml) under Ar, (*i*Pr)$_2$EtN (0.27 ml, 1.55 mmol) and 2-cyanoethyl diisopropylphosphoramidochloridite (260 µl, 1.14 mmol) were added, and the mixture was stirred at r.t. for 30 min. The reaction was monitored by TLC. The mixture was diluted with $CH_2Cl_2$ and the soln. washed with 5% aq. $NaHCO_3$ soln. and brine. The org. phase was dried ($Na_2SO_4$) and evaporated and the product separated by FC (2.5 cm × 6 cm, *D*): **11** (0.5 g, 66%). Colorless foam. $R_f$ (*E*) 0.50, 0.59. $^1$H-NMR ((D$_6$)DMSO): 1.10 (*m*, *Me*$_2$CH); 2.44 (*m*, 1 H–C(2′)); 2.64 (*m*, Me$_2$C*H*); 2.99 (*m*, 1 H–C(2′), 2 H–C(5′)); 3.36 (*m*, C$H_2$C$H_2$); 3.78 (*s*, 2 MeO); 4.32 (*m*, H–C(4′)); 4.74 (*m*, H–C(3′)); 6.35 (*m*, H–C(1′)); 6.74–7.35 (*m*, arom. H); 8.28 (*s*, H–C(7)); 9.15 (*s*, NH). $^{31}$P-NMR ($CDCl_3$), 150.22, 150.50.

## REFERENCES


[1] F. Seela, H. Steker, *Helv. Chim. Acta* **1985**, *68*, 563.
[2] F. Seela, M. Zulauf, H. Debelak, *Helv. Chim. Acta* **2000**, *83*, 1437.
[3] F. Seela, M. Zulauf, *J. Chem. Soc., Perkin Trans. 1* **1998**, 3233.
[4] F. Seela, H. Debelak, *Nucleic Acids Res.* **2000**, *28*, 3224.
[5] F. Seela, K. Kaiser, *Helv. Chim. Acta* **1988**, *71*, 1813.
[6] F. Seela, H. Debelak, *J. Org. Chem*. **2001**, *66*, 3303.
[7] F. Seela, G. Becher, *Nucleic Acids Res.* **2001**, *29*, 2069.
[8] C. Cheong, I. Tinoco, J. A. Chollet, *Nucleic Acids Res.* **1988**, *16*, 5115.
[9] F. Seela, G. Becher, *Synthesis* **1998**, *2*, 207.
[10] I. Luyten, A. V. Aerschot, J. Rozenski, R. Busson, P. Herdewijn, *Nucleosides Nucleotides* **1997**, *16*, 1649.
[11] G. Becher, J. He, F. Seela, *Helv. Chim. Acta* **2001**, *84*, 1048.
[12] V. Boudou, L. Kerremans, B. De Bouvere, E. Lescrinier, G. Schepers, R. Busson, A. Van Aerschot, P. Herdewijn, *Nucleic Acids Res.* **1999**, *27*, 1450.
[13] G. S. Ti, B. L. Gaffney, R. A. Jones, *J. Am. Chem. Soc*. **1982**, *104*, 1316.
[14] Y. S. Sanghvi, G. D. Hoke, S. M. Freier, M. C. Zounes, C. Gonzalez, L. Cummins, H. Sasmor, P. D. Cook, *Nucleic Acids Res.* **1993**, *21*, 3197.
[15] H. Rosemeyer, G. Toth, B. Golankiewicz, Z. Kazimierczuk, W. Bourgeois, U. Kretschmer, H.-P. Muth, F. Seela, *J. Org. Chem*. **1990**, *55*, 5784.
[16] J. van Wijk, C. Altona, 'PSEUROT 6.2 – A Program for the Conformational Analysis of the Five-Membered Rings', University of Leiden, July, 1993.
[17] H. Rosemeyer, M. Zulauf, N. Ramzaeva, G. Becher, E. Feiling, K. Mühlegger, I. Münster, A. Lohmann, F. Seela, *Nucleosides Nucleotides* **1997**, *16*, 821.
[18] E.-I. Suzuki, N. Pattabiraman, G. Zon, T. L. James, *Biochemistry* **1986**, *25*, 6854.
[19] B. L. Gaffney, L. A. Marky, R. A. Jones, *Nucleic Acids Res.* **1982**, *10*, 4351.
[20] J. A. McDowell, D. H. Turner, *Biochemistry* **1996**, *35*, 14077.


*Received November 19, 2001*